Original Article

The Study of Apoptosis-inducing Effects of Three Pre-apoptotic Factors by Gallic Acid, Using Simulation Analysis and the Comet Assay Technique on the Prostatic Cancer Cell Line PC3

Javad Saffari-Chaleshtori[1], Ehsan Heidari-Sureshjani[2], Fahimeh Moradi[3], Hojjatollah Molavian Jazi[4], Esfandiar Heidarian[1]

[1] *Clinical Biochemistry Research Center, Basic Health Sciences Institute, Shahrekord University of Medical Sciences, Shahrekord, Iran*

[2] *Young Researchers and Elites Club, Islamic Azad University, Shahrekord Branch, Shahrekord, Iran*

[3] *Cellular and Molecular Research Center, Basic Health Sciences Institute, Shahrekord University of Medical Sciences, Shahrekord, Iran*

[4] *Department of Biochemistry, Islamic Azad University Branch of Sanandaj, Sanandaj, Iran*

Submitted: 28 Sep 2016
Accepted: 18 May 2017
Online: 18 Aug 2017

To cite this article: Saffari-Chaleshtori J, Heidari-Sureshjani E, Moradi F, Jazi HM, Heidarian E. The study of apoptosis-inducing effects of three pre-apoptotic factors by Gallic acid, using simulation analysis and the comet assay technique on the prostatic cancer cell line PC3. *Malays J Med Sci.* 2017;**24(4)**:18–29. https://doi.org/10.21315/mjms2017.24.4.3

To link to this article: https://doi.org/10.21315/mjms2017.24.4.3

Abstract

***Background*: In this study, we demonstrated the effects of the Gallic Acid (GA) molecule on the prostate cancer cells line PC3 using the comet assay (Alkaline electrophoresis) technique and its effects on some important apoptotic factors including BAD (Bcl-2-Associated Death promoter), BAK (Bcl-2 homologous Antagonist/Killer), and BIM (Bcl-2-like protein 11) via simulation analysis by using the Auto Dock and Gromacs software.**

***Methods*: Following the MTT assay on the PC3 cells, and determining IC50, we used three concentrations of GA to around IC50 to treat PC3 cells. 100 comet pictures were obtained by alkaline electrophoresis and have been analysed with the CASP version 1.2.2 software; all the results were thereafter analysed by the SPSS version 21 statistical software.**

***Results*: The IC50 value for GA was determined to be 35 µM. The ratio of tail to head in alkaline electrophoresis for the three concentrations below the IC50 of GA in 25, 30, and 35 µM were measured as 24.7 (2.7), 44.5 (1.8), and 57.3 (1.3) percent, respectively. The results of the pre-apoptotic factors (BAD, BAK, and BIM) in the performed simulation in the absence and presence of GA showed that the GA protein causes the structural instability in the BAD protein, and the effect of GA can be explained by the creation of hydrogen bonds with proteins.**

***Conclusion*: GA is a polyphenol compound in plants that can suppress cell growth and induce apoptosis in PC3 cells in prostate cancer in the range of IC50 concentrations. The apoptotic properties of GA induce pre-apoptotic factors.**

Keywords: *simulation, apoptosis, gallic acid*

Introduction

The importance of antioxidants and polyphenols in the prevention or inhibition of many dangerous diseases, such as cancers and degenerative disorders, is well known today. Among them, Gallic acid (GA) (3,4,5-trihydroxybenzoic acid), C6H2(OH)3COOH or C7H6O5, is one of the most prominent compounds (1). This benzoic acid ring containing polyphenol (Figure 1) has a Molecular Weight (MW) of 170.11954 g/mol, a melting point of 250 °C, and 1.1% water solubility at 20 °C. GA is a plant polyphenol abundantly found in fruits like berries and grapes, hard wood plant species such as chestnut (Castanea sativa L.) and oak (Quercus robur), and also in tea. This yellowish white crystal is known to affect several biochemical pathways with strong antioxidant activity (2–5).

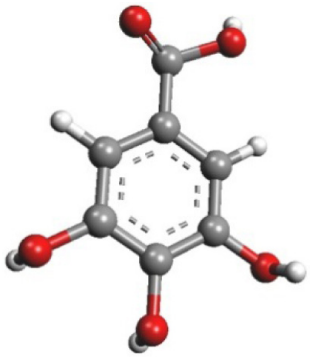

Figure 1. Molecular structure of Gallic Acid (GA)

Indeed, it has been demonstrated that GA has a concentration dependent pro-oxidant property, requiring metal ions. This property has been linked to the apoptosis-inducing activity in cancer cell lines. Similarly, recent studies have shown a cytoprotective feature for GA against chemically-induced carcinogenesis (6, 7). The diverse effects of GA on various tumour types have been well studied at different molecular levels. Its anti-cancer activities including the selective cytotoxicity for cancerous cells and the low cytotoxicity for normal cells, introduce GA as an important biomolecule and a suitable compound for therapeutic aims. GA shows the selective cytotoxicity of cancerous cells and also has a lower cytotoxicity among normal cells (8). It has been well documented that GA can induce apoptosis in 3T3-L1 preadipocytes; furthermore, there is evidence to suggest that GA can activate ATM kinase and act as an anti-carcinogenesis in the DU145 prostatic cancer cell line (9, 10). Furthermore, studies have shown that GA inhibits the Ribonucleotide reductase. This inhibition can result in the alteration of the deoxy Nucleotide Triphosphate (dNTP) level, especially by decreasing the concentration of intracellular dATP and dGTP (11). Another important role of GA against carcinogenesis is the inhibitory effect of GA on Cyclooxygenase-2 (COX-2) in K562 and IR-K562 cells, which is in concordance with the fact that GA can inhibit the UDP-glucose dehydrogenase (UGDH) enzyme, and therefore, interfere in the conversion of UDP-glucose to UDP-glucuronate by NAD+-dependent two-step oxidation in MCF-7 breast carcinomas (12, 13). Anti-angiogenic effects (14), NF-κB inhibition(15), and other effects of GA (16, 17) showed that this antioxidant plays important roles in cells. There are many factors that can affect apoptosis as well. BAD, BAK, and BIM are three factors that initiate the apoptosis cascade in cells (18–20). The aim of this study is the investigation of the effects of GA on the prostatic cancer (PC3) cell line using the comet assay (alkaline electrophoresis) technique. We have also performed in-silico studies to determine the effects of GA on some important apoptotic factors such as BAK, BID, and BIM via simulation studies.

Materials and Methods

Laboratory Studies

Cell culture

The prostatic cancer cell line PC3 was purchased from the Institute Pastor Centre (Tehran, Iran). The cells were cultured in the RPMI medium supplemented with 10% FBS, 2 mM glutamine, and 1% (100 µg/ml/100 U/ml) penicillin/streptomycin antibiotics.

MTT Assay

The cells were seeded in a multi-well plate containing 150 × 103 cells/ml, cultured in the RPMI medium supplemented with 10% FBS, 2 mM glutamine, and 1% (100 µg/ml/100 U/ml) penicillin/streptomycin antibiotics; the cells were allowed to attach for 24 hours at 37 ºC in a CO2 incubator. The liveability of the cells in various concentrations of GA were detected by the MTT [3-(4,5-dimethylthiazol-2-yl)-2,5-diphenyl-terazolium bromide] (BIO-IDEA) assay kit; the IC50 was also determined. Three

concentrations below the IC50 were chosen to be used in the comet assay.

Comet Assay

Positive control

Positive control PC3 cells were treated with 30 μM H2O2 according to the method described by Benhusein et al. (21).

The Alkaline Comet Assay

The alkaline comet assay was performed according to standard protocol described by McKelvey-Martin et al. (22) with a few modifications.

Statistical analysis

Each experiment was performed at least three times. The data was analysed using a statistical package for the Social Sciences software, version 22 (SPSS, Inc., Chicago, IL, USA). The alkaline comet assay parameters were evaluated by the CaspLab software version 1.0.0. The differences between the alkaline comet assay parameters were analysed using the repeated measures of the ANOVA test for comparing the significant difference among the means of the various concentrations. P-values less than 0.001 were considered statistically significant.

Simulation Studies

Getting PDB files

To develop molecular structures, the Protein Data Bank file of BAD, BAK, and BIM proteins (with ID: 1G5J ID: 1BXL, and ID: 1PQ1, respectively) as the three important factors in cells apoptosis process were obtained from www.rcsb.org. The three-dimensional structure of GA was obtained from ChEMBL and converted into a PDB file by the Mercury 3.6 software. The GA has also been structurally optimised by the ArgusLab software.

Protein Molecular Dynamic Simulation

The survey of the molecular dynamics simulation of the three proteins (BIM, BAD, and BAK), which were accomplished in pure water, showed related structures undergoing variations in temperature and pressure; a concentration of 140 mMol was required to reach a state of equilibrium. Three pre-apoptotic studied factors (BIM, BAD, and BAK) were simulated by the Gromacs 4.6.1 software using an aqueous solvent with the SPC216 water model and the G43A1 force field (23). In this study, the SPC216 model was used. When the system reaches a concentration of 140 mM, an adequate number of Na and Cl ions were added instead of the solvent. To perform the simulation and to maximize the energy, the steepest descent algorithm and an integration of 50,000 steps were used. Then, the equilibration steps were performed using the NVT and the NPT ensembles by means of the LINCS algorithm for an integration of 50,000 steps. The configuration of each system was saved at 0.2 PS intervals. Fixation was performed for all the bonds. The main sampling was performed using the NPT ensemble within 30 ns. To fix the temperature and the pressure of the system at 300 kelvin and one bar, the V-rescale thermostat and Parrinello–Rahman Barostat were used. The length of the bonds including the hydrogen atom was fixed by the LINCS algorithm. For long distance electrostatic interactions, the particles with 1 nm diameter were subjected to the Particle Mesh Ewald method of integration; the Newton Movements Equations were used by a half-step leap and the time step was set to 2 fs. The saved routes in the simulation were used as controls to analyse the structural parameters of the BIM, BAD, and BAK proteins in the presence of a ligand (24).

Docking

The output PDB files were simulated in water on the basis of the method of molecular docking discussed below. The AutoDock 4.1 software was employed to dock the small molecules in macromolecules. This software predicts how a substrate or a drug is docked in the receptor and how its three-dimensional structure is demonstrated. The GA was docked next to the aforementioned pre-apoptotic factors discussed and they were assessed by the software. To attribute the bar to the protein, Kollman bars were used; for the ligand, Gasteger bars were used. The used grid limiting the docking area included all the volume of the protein. To perform docking, a genetic algorithm was used and the highest number of value was 200 (25).

Protein-ligand Molecular Dynamic Simulation

After docking, the hydrogen and the hydrophobic bonds between GA and the three pre-apoptotic factors were derived by the Ligplot software. Furthermore, after the docking results were derived for the three pre-apoptotic factors,

the simulation was accomplished according to the simulation of molecular dynamics in the presence of GA. Finally, the molecular dynamics simulation of the complex of all three proteins (BIM, BAD, and BAK) with the GA ligand was performed in the aqueous solution as per the above method and the saved routes in simulation were used to analyse the structural parameters of the complex (23).

Results

The MTT assay results

The different concentrations (between 0–1000 µM) of GA were used on prostatic cancer cells line PC3. The IC50 of these concentrations was determined to be about 35 µM according to MTT assay results. High concentrations of GA can give rise to cell death. In lower concentrations such as 35 µM of GA, 50 percent of cells were alive. In lower concentrations such as 30 µM and 25 µM of GA above 60 percent of cells survived. In Figure 2, the percentage of viability the various concentrations of (GA) on prostatic cancer cells line PC3 has been shown. The analysis showed that there was significant relationship between the concentration of the GA and cell death.

The Comet Assay Results

The details of the alkaline comet assay analysis on the prostatic cancer cell line PC3 with various concentrations of GA (25, 30 m, and 35 µM GA) have been shown in Table 1. The rate of the tail comet to head comet (Tail DNA %) percentage in alkaline electrophoresis for the three concentrations below the IC50 of GA in 25, 30, and 35 µM were 24.7 (2.7), 44.5 (1.8) and 57.3 (1.3) percent, respectively. In this study, we used the prostatic cancer cell line PC3 treated with 50 µM of H2O2 as positive control and the prostatic cancer cell line PC3 without treatment (0 µM of GA) as negative control.

Head area: area of the comet head in pixels, Tail area: area of the comet tail in pixels, Head DNA: amount of DNA in the comet head, Tail DNA: amount of DNA in the comet tail, Head DNA%: percent of DNA in the comet head to comet tail, Tail DNA%: percent of DNA in the comet tail to comet head, Head Radius: Radius of the comet head (in pixels), Tail Length: length of the comet tail measured from right border of head area to end of tail (in pixels), Comet length: length of the entire comet from left border of head area to end of tail (in pixels), Head Mean X: Center of gravity of DNA in the head (x coordinate), Tail Mean X: Center of gravity of DNA in the tail (x coordinate), Tail moment: tail DNA % x tail length [(percent of DNA in the tail) x (tail length)]. The data has been shown as mean)SD). A, B, C, and D are treated groups with 0, 25, 30, and 35 µM of Gallic Acid and E is positive control, a treated group with 50 µM H2O2. This data analysed by repeated measure ANOVA.

(a) $P < 0.001$ compared with group A

(b) $P < 0.001$ compared with group B

(c) $P < 0.001$ compared with group C

(d) $P < 0.001$ compared with group D

The *P*-value for the tail DNA% factor between the negative control group and other groups (25, 30, 35 µM, and positive control) as well as between the groups were calculated as less than 0.001.

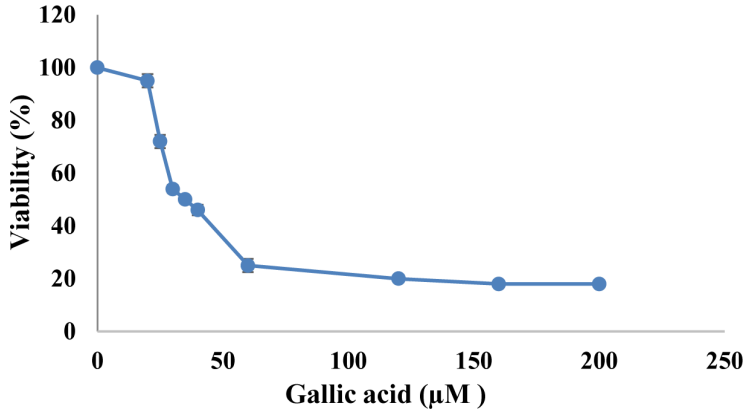

Figure 2. Percent of viability the various concentrations of Gallic Acid (GA) on prostatic cancer cells line PC3. In concentrations of 25 and 30 µM of Gallic acid above the 60 percent cells were live

Table 1. The details of alkaline comet assay analysis on prostatic cancer cell line PC3 with various concentrations of Gallic acid (µM).

Groups Parameter	*n*	A	B	C	D	E
Head Area	100	349.5(59.1)	1148.7(191)^{a}	2325.6(622)^{ab}	265.5(76.6)^{abc}	357.9(2.7)^{bcd}
Tail Area	100	41.2(18.1)	917.8(22.5)^{a}	2820.3(602)^{ab}	776.9(110.9)^{abc}	1821.4(265)^{abcd}
Head DNA	100	35.4(5.3)	79.39(13.4)^{a}	99.1(42.4)^{ab}	12.5(2.5)^{abc}	27.1(13.0)^{abcd}
Tail DNA	100	1.1(0.5)	25.9(4.8)^{a}	78.8(32.3)^{ab}	16.8(3.4)^{abc}	68.1(17.5)^{abcd}
Head DNA%	100	97.2(1.2)	75.3(2.7)^{a}	55.5(1.8)^{ab}	42.7(1.3)^{abc}	27.2(5.7)^{abcd}
Tail DNA%	100	2.8(1.2)	24.7(2.7)^{a}	44.5(1.8)^{ab}	57.3(1.3)^{abc}	72.8(5.7)^{abcd}
Head Radius	100	10.3(0.9)	18.8(1.3)^{a}	26.7(4.2)^{ab}	8.9(1.3)^{abc}	10.7(3.7)^{bcd}
Tail Length	100	4.1(1.2)	17.8(2.9)^{a}	35.3(5.5)^{ab}	32.8(3.6)^{ab}	44.9(3.3)^{abcd}
Comet Length	100	25.7(2.6)	56.5(4.1)^{a}	89.7(13.1)^{ab}	51.7(2.6)^{abc}	67.3(9.8)^{abcd}
Head Mean X	100	1.1(0.1)	86.2(1.3)	29.1(0.4)^{ab}	42.5(1.4)^{c}	32.6(3.0)^{abcd}
Tail Mean X	100	349.5(3.2)	136.9(1.3)^{a}	54.3(0.1)^{ab}	69.9(2.1)^{ac}	356.9(3.4)^{acd}
Tail Moment	100	1.1(0.1)	4.5(1.1)^{a}	15.7(2.4)^{ab}	18.8(2.1)^{abc}	32.6(3.0)^{abcd}
OliveTailMoment	100	35.4(2.1)	7.0(0.1)^{a}	10.3(0.2)^{ab}	13.4(0.5)^{ab}	27.1(1.3)^{abcd}

The rate of tail comet to head comet is increases with the increase of GA concentration. A comparative chart of the percent of DNA in the comet tail to the comet head in the PC3 cell line treated with various concentrations of GA is shown in Figure 3.

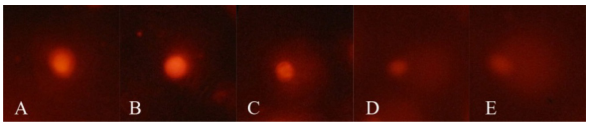

Figure 3. Percent of DNA in the comet tail to comet head (Tail DNA %). A: PC3 cells line without treatment (Control –). B: PC3 cells line treated with 25 µM GA. C: PC3 cells line treated with 30 µM Gallic acid. D: PC3 cells line treated with 35 µM Gallic acid. E: PC3 cells line treated with 50 µM H2O2 (Control +)

The rate of the tail comet to the head comet is increased with the increase of GA concentration. A comparative chart of the percent of DNA in the comet tail to the comet head in the PC3 cell line treated with various concentrations of GA is shown in Figure 4.

The Computational Results

In this study, we used the molecular dynamic to detect the effect of GA on BIM, BAD, and BAK pre-apoptotic factors.

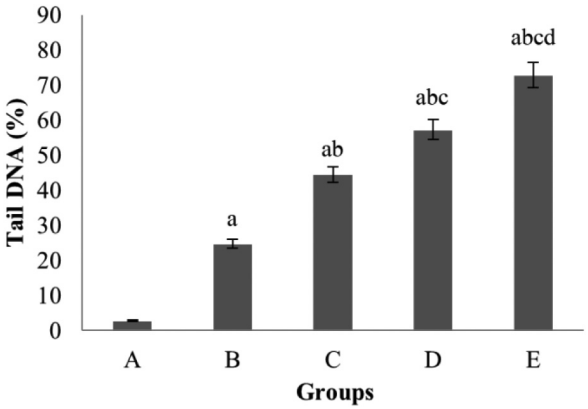

Figure 4. Percent of DNA in the comet tail to comet head (Tail DNA %)

Molecular Docking Study

To evaluate the effect of the GA compound on apoptotic factors including BIM, BAK, and BAD, the molecular docking approach was adopted. In the docking method, the most presumable sites of interaction on the three pre-apoptotic factors (BIM, BAK, and BAD) were obtained, and then, they were scored according to the energy rating index. Table 2 indicates the results of molecular docking, and in Figure 5, hydrogen and hydrophobic bonds indicate that GA has bonding energy equal to −6.97, −6.8 and −5.7 with BAD, BAK, and BIM, respectively. A comparison of these binding energies revealed that GA has the most potential to bind to BAD in comparison to the other studied factors. Moreover, the results indicated that the Van der Waals forces are more involved in binding in comparison to the electrostatic forces.

Table 2. The results of molecular docking of GA on tree pre-apoptotic factors BAD, BAK and BIM.

Complex	BE	FIE	EIC	Interaction bonds	
				Hydrogen Bonding	Hydrophobic Bonding
BAD-Gallic acid	-5.56	-7.35	84.59	Ser47, Ser8, Glu43, Glu46, Gly44, Pro42, Trp192	Ser47, Ser8, Glu43, Glu46, Gly44, Pro42, Trp192
BAK-Gallic acid	-4.65	-6.46	388.51	Asp54, Val58,Ilu59, Leu60, Gly149, Leu148, Phe147, Gly146	Asp54, Val58,Ilu59, Leu60, Gly149, Leu148, Phe147, Gly146
BIM-Gallic acid	-4.39	-6.18	605.28	Asp66, Lys62, Lys63, Met1, Asp64, Ser67	Asp66, Lys62, Lys63, Met1, Asp64, Ser67

BE: Binding and Energy (kcal/mol) FIE: Final Intermolecular energy (kcal/mol), EIC: Estimated Inhibition Constant (μM), Interaction bonds contain the number of amino acids with hydrogen bonding and hydrophobic bonding. The data has been shown the lowest level of energy in binding site.

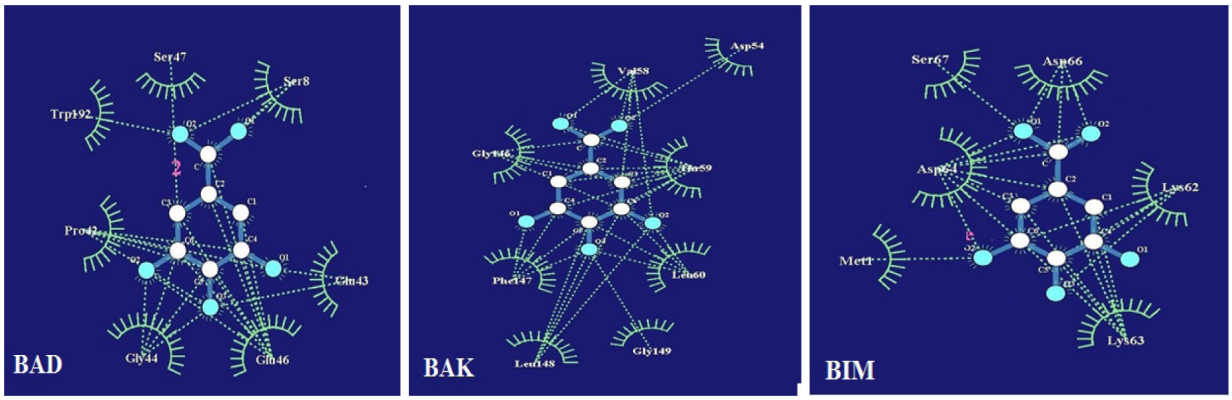

Figure 5. Hydrogen and hydrophobic bonds of GA in interaction with pre-apoptotic factors BAD, BAK, BIM residues by Ligplot software

Interaction tendency of GA with BAD, BAK, and BIM was evaluated in 200 steps. Finally, their binding site was recognised in the lowest status of energy. Figure 6 demonstrates this position for the compound in the studied factors.

Molecular Dynamic (MD) Simulation

In Figure 7, the changes in the potential and the kinetic energy at the length of 10 ns has been demonstrated, leading to the inference that all the three proteins had a structural balance during the simulation time and they have a steady interaction structurally. According to Figure 7, the potential and kinetic energy in the opposite or the same direction varies during 10 ns. A low standard deviation of total or potential energy demonstrated that the law of conservation of energy is established in the

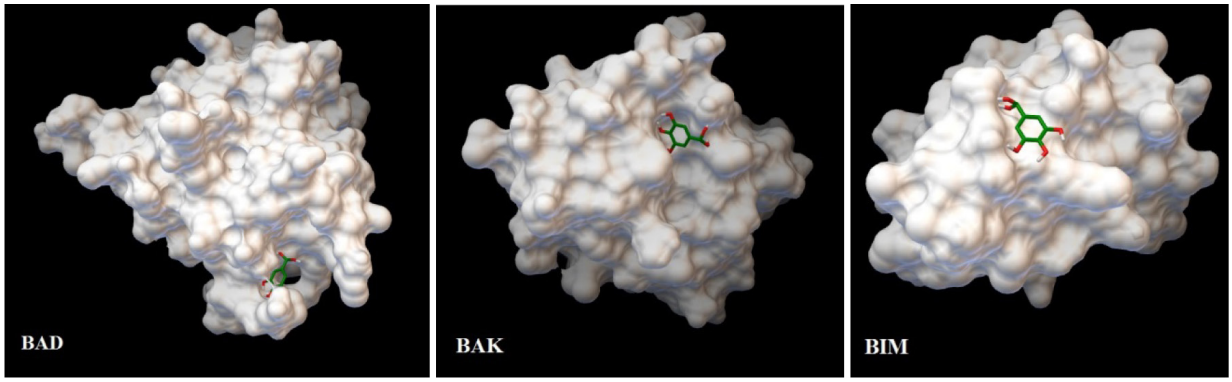

Figure 6. The position of GA on three-dimensional structures of BAD, BAK, and BIM

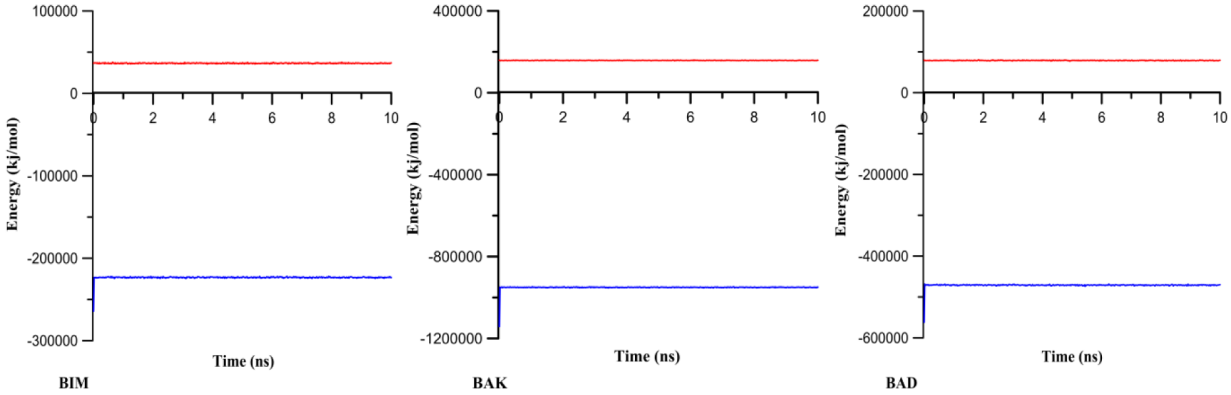

Figure 7. Potential and synthetic energy of system during 10 ns of the production run simulations. (Red color indicates simulation in water. Blue color shows simulation of proteins and GA)

system. The potential and kinetic energy oscillate in the same or the opposite direction during the 10 ns of simulation (Figure 7). The lower rate of standard deviation of the total and the potential energy revealed that the law of energy conservation is established within the system.

Table 3 demonstrates the Root-Mean-Square Deviation (RMSD) of the main skeleton of apoptotic proteins. Radius Gyration (RG), temperature, potential and kinetic energy, and the number of hydrogen bonds between apoptotic proteins and the water molecules as well as between the apoptotic proteins and the GA during the 10 ns of molecular dynamic simulation were measured. These results signify that the tendency of GA to bind to BAD is higher in comparison to the other two factors.

P < 0.001 Compared with G1

The RMSD of the main skeleton of the apoptotic proteins BAK, BAD, and BIM is derived in the presence and the absence of GA as reference. The results in Figure 8 indicate that in the last 4 ns, the RMSD of the main skeleton of apoptotic proteins including BAK, BAD, and BIM in the absence of GA is 0.3367 (0.0156), 0.2175 (0.0243), and 0.4190 (0.0180) nm, respectively; in the presence of GA, it is 2.34 (0.21), 0.3873 (0.0144), and 3.1999 (0.3204) nm, respectively. These results demonstrate that the proteins become immediately balanced structurally in the absence of GA. In the presence of GA, however, the apoptotic proteins become structurally unbalanced and become a stable structure during a longer time, implying that GA has affected their structure.

In Figure 9, the Root-Mean-Square Fluctuation (RMSF) changes of the amino acids of apoptotic proteins demonstrate the total flexibility of the proteins in the presence and the absence of GA. Subtle changes of amino acids of BAD as an apoptotic protein in the presence or the absence of GA demonstrates the stability of structure of this protein during simulation which indicates the tendency of this factor to GA without any tangible change in its

Table 3. The changes of the mean of RG, kinetic, temperature, potential, hydrogen-bonding between of protein and protein

Protein		Rg	TE	RMSF	RMSD	AP	AK
BAD	G1	1.61(0.01)	-208258(722)	0.16(0.12)	0.42(0.02)	-256292(528)	48034(408)
	G2	1.60(0.01)[a]	-392085 (922)[a]	0.16(0.1)	2.34(0.21)[a]	-470944(728)[a]	78858(515)[a]
BAK	G1	1.44(0.01)	-127646(789)	0.15(0.10)	0.34(0.01)	-157154(463)	29511(530)
	G2	1.43(0.01)[a]	-792351(1151)[a]	0.12(0.07)[a]	0.39(0.01)	-950299(925)[a]	157948(655)[a]
BIM	G1	1.19(0.01)	-89911(471)	0.20(0.13)	0.22(0.02)	-109680(355)	19768(267)
	G2	1.19(0.01)	-186670(605)[a]	0.12(0.07)[a]	3.20(0.32)[a]	-223228(471)[a]	36548(341)[a]

Rg: radius of gyration. TE: Total Energy. AT: Average Temperature (K): AK: Average kinetic: AP: Average Potential) KJ/mol (G_1: factors Simulation before Docking. G_2: factors Simulation after Docking. The data has been shown as mean (SD).

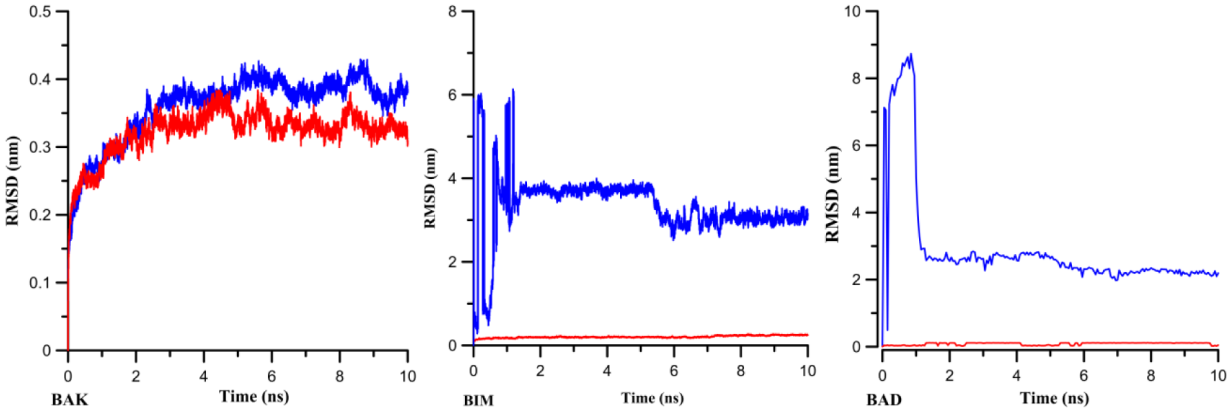

Figure 8. Changes in root-mean square displacement of main skeleton of apoptotic protein (BAK, BIM, BAD) in the presence and the absence of GA. Red color curve is indicating the simulation of protein in water. Blue color curve is indicating the protein simulation and GA

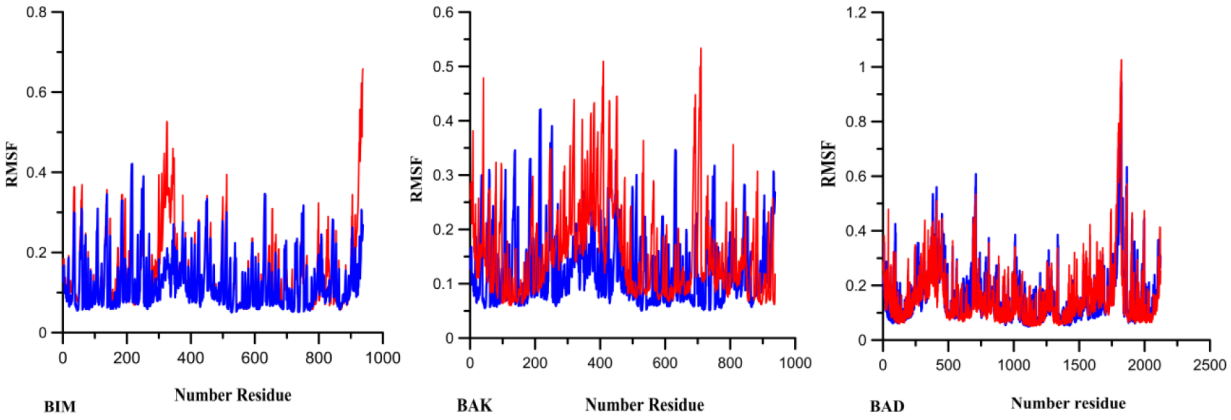

Figure 9. RMSF of apoptotic proteins (BAK, BIM, BAD) in the presence and the absence of GA. Red color curve is indicating the simulation of protein in water. Blue color curve is indicating the protein simulation and GA

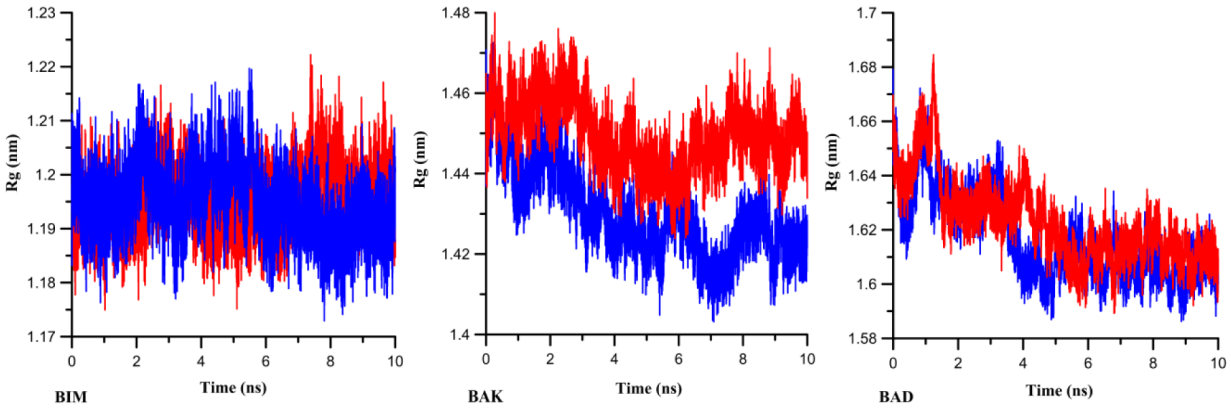

Figure 10. Protein-protein Rg for BAK, BAD, BIM. Red –color curve: protein simulation in water. Blue color: protein simulation with GA

structure (Table 2). Figure 9 shows that changes in the RMSF of amino acids of the apoptotic proteins indicates the general flexibility of proteins in the presence and the absence of GA. Subtle changes in the amino acids of BAD as an apoptotic protein in the presence and the absence of GA suggest the structural stability of this protein during simulation; this is regarded as the tendency of BAD towards GA without the necessity to change its structure.

The protein–protein RG for BAK, BAD, and BIM is shown in Figure 10 and the numerical values of the RG difference between the presence and the absence of GA is shown in Table 3.

Discussion

There are many studies that introduce antioxidants and plant polyphenols with the ability to inhibit and decrease tumour cell growth (26). Some studies have revealed that these compounds can enhance apoptosis in cancer cells (27): GA is one of these compounds that has attracted the attention of many studies (1). Yong et al. showed that GA can reduce cell viability, proliferation, invasion, and angiogenesis in human glioma cells (17). Yeh et al. reported that GA induces G0/G1 phase arrest and apoptosis in human Leukaemia HL-60 cells through inhibiting Cyclin D and E, and activating the mitochondria-dependent pathway (28). In the present study, the effects of GA as an antioxidant on the PC3 cell line have been evaluated. Increasing concentrations of GA enhanced the genome breakage in the cells so that the IC50 concentration had the maximum effect over the genome. The tail to head ratio is an appropriate criterion in determining the frequency of breakage that was measured by using the version 1.2.2 CASP software (29, 30). The ratio of tail to head over 10% was regarded as minor damage, whereas higher ratios indicated major genome damage (31). Positive control (samples treated with 50 μM H2O2) had the tallest tail (72.8 ± 5.7), whereas the most damaging effect of GA over the PC3 cell line were in the IC50 concentration (35 μM) that was measured as 57.3 ± 1.3. The head to tail ratio in lower concentrations were equal to 30 μM (44.5 ± 1.8) and 25 μM (24.7 ± 2.7) as calculated. The tail to head ratio in negative controls (cells without treatment) was 2.8 ± 1.2. The most optimum concentration in comet assay was IC50; higher concentrations lead to cell death. In this study, 35 μM concentration of GA had the most damaging effect on the PC3 cell line. This damage can be exerted due to apoptosis induction. Programmed cell death will occur when the cell factors are involved in the apoptosis pathway activation. In this condition, the cell tumours will be inactive and the cancer cells will be destroyed (32, 33). Among the critical factors, Bcl2 plays a key role in the control and the induction of apoptosis that inhibits carcinogenesis in normal cells (34). Bcl2 activation induces many pre-apoptotic factors including BAX, BIM, BAK, BAD, BIK, and BID (35). These pre-apoptotic factors affect the mitochondria membrane thus activating the caspases through the cytochrome c activation, and finally giving rise to a death signal for the cell (36, 37). Since many factors involved in apoptosis pathway play a key role in the induction or suppression of this process, in this study the molecular dynamic properties of the three pre-apoptotic molecules (including BIM, BAK and BAD) in the presence of GA as a very effective flavonoid was investigated. Surveying the effect of Hesperetin over the pre-apoptotic factors in simulation situation, Shanmugam et al. reported that Hesperetin can activate BAX and BAD, and suppress NF-κB (38). The same studies in the simulated environment revealed that carvacerol can potentially activate pre-apoptotic factors including BAK, BAD, and BID—and most of all, BIM (39). According to Saffari et al., in a study accomplished in a simulated environment, quercetin has the potential to activate pre-apoptotic factors like BIM, BAD, and especially BAD (40). Precise simulation results of GA associated with GA have been presented in Table 3. During the docking process, hydrogen bonds between Ser47, Ser8, Glu43, Glu46, Gly44, Pro42, and Trp192 residues and BAD were established. In addition, Asp54, Val58, Ilu59, Leu60, Gly149, Leu148, Phe147, Gly14, Asp66, Lys62, Lys63, Met1, Asp64, and Ser67 bonds with BAK and BIM were established. According to the present study, it can be concluded that GA bonds with the apoptotic proteins and affects their function. The molecular dynamic simulation accomplished to acquire the complex models is in a close state to the normal condition. The results obtained from the molecular dynamic simulation demonstrate a stable status in the mode of the ligand–receptor bond during molecular docking. The results of molecular docking and dynamic confirmed that GA can be considered as a potential ligand for BIM, BAD, and BAK, among which the bonding between GA

and BAD is the strongest. In this study, we saw that GA could increase the genome decline and induce cell death at an IC50 concentration.

Conclusion

Recently, many studies have focused on identification as well as determining the function of inhibitors and natural activators. According to our finding, GA could increase genome damage and also induce cell death at the range of IC50 concentration. The results obtained from the molecular dynamic studies introduced GA as an effective factor to control pre-apoptotic proteins including BAK, BAD, and BIM; GA can, therefore, be used to treat many tumour cells effectively.

Acknowledgements

This paper was based on a research project (number: 2193) funded by the Deputy of Research and Technology of the Shahrekord University of Medical Sciences, Shahrekord, Iran. We gratefully thank the Deputy and also to The RayaZist Company, Shahrekord, CHB, Iran for Bioinformatics support.

Authors' Contributions

Conception and design: EH-S. JS-C
Drafting of the article: EH-S, IS-C, EH
Final approval of the article: EH
Provision of study materials or patients: FM, HM
Administrative, technical, or logistic support: FM, HM
Collection and assembly of data: EH-S. JS-C

Correspondence

Dr Ehsan Heidari-Sureshjani
MsC (Islamic Azad University, Shahrekord Branch, Shahrekord)
Young Researchers and Elites Club,
Islamic Azad University,
Shahrekord Branch,
Shahrekord 8815713471
Iran (the Islamic Republic of).
Tel: +98 38 3336 1000
Fax: +98 38 3336 1010
E-mail: j_saffari@yahoo.com

References

1. Locatelli C, Filippin-Monteiro FB, Creczynski-Pasa TB. Alkyl esters of gallic acid as anticancer agents: a review. *European Journal of Medicinal Chemistry*. 2013;**60**:233–239. https://doi.org/10.1016/j.ejmech.2012.10.056

2. Singh J, Rai G, Upadhyay A, Kumar R, Singh K. Antloxldant phytochemicals in tomato (Lycopersicon esculentum). *Indian Journal of Agricultural Science*. 2004;**74(1)**:3–5. http://cat.inist.fr/?aModele=afficheN&cpsidt=15634188

3. Eyles A, Davies N, Mitsunaga T, Mihara R, Mohammed C. Role of Eucalyptus globulus wound wood extractives: evidence of superoxide dismutase-like activity. *Forest Pathology*. 2004;**34(4)**:225–232. https://doi.org/10.1111/j.1439-0329.2004.00361.x.

4. Murugananthan M, Bhaskar Raju G, Prabhakar S. Removal of tannins and polyhydroxy phenols by electro-chemical techniques. *Journal of Chemical Technology and Biotechnology*. 2005;**80(10)**:1188–1197. https://doi.org/10.1002/jctb.1314

5. Kim D-O, Lee KW, Lee HJ, Lee CY. Vitamin C equivalent antioxidant capacity (VCEAC) of phenolic phytochemicals. *Journal of Agricultural and Food Chemistry*. 2002;**50(13)**:3713–3717. https://doi.org/10.1021/jf020071c

6. Senapathy JG, Jayanthi S, Viswanathan P, Umadevi P, Nalini N. Effect of gallic acid on xenobiotic metabolizing enzymes in 1, 2-dimethyl hydrazine induced colon carcinogenesis in Wistar rats–a chemopreventive approach. *Food and Chemical Toxicology*. 2011;**49(4)**:887–892. https://doi.org/10.1016/j.fct.2010.12.012

7. Padma VV, Sowmya P, Felix TA, Baskaran R, Poornima P. Protective effect of gallic acid against lindane induced toxicity in experimental rats. *Food and Chemical Toxicology*. 2011;**49(4)**:991–998. https://doi.org/10.1016/j.fct.2011.01.005

8. Chia Y-C, Rajbanshi R, Calhoun C, Chiu RH. Anti-neoplastic effects of gallic acid, a major component of Toona sinensis leaf extract, on oral squamous carcinoma cells. *Molecules*. 2010;**15(11)**:8377–8389. https://doi.org/10.3390/molecules15118377

9. Hsu C-L, Huang S-L, Yen G-C. Inhibitory effect of phenolic acids on the proliferation of 3T3-L1 preadipocytes in relation to their antioxidant activity. *Journal of Agricultural and Food Chemistry*. 2006;**54(12)**:4191–4197. https://doi.org/10.1021/jf0609882

10. Hsu C-L, Lo W-H, Yen G-C. Gallic acid induces apoptosis in 3T3-L1 pre-adipocytes via a Fas-and mitochondrial-mediated pathway. *Journal of Agricultural and Food Chemistry*. 2007;**55(18)**:7359–7365. https://doi.org/10.1021/jf071223c

11. Madlener S, Illmer C, Horvath Z, Saiko P, Losert A, Herbacek I, et al. Gallic acid inhibits ribonucleotide reductase and cyclooxygenases in human HL-60 promyelocytic leukemia cells. *Cancer Letters*. 2007;**245(1)**:156–162. https://doi.org/10.1016/j.canlet.2006.01.001

12. Reddy TC, Reddy DB, Aparna A, Arunasree KM, Gupta G, Achari C, et al. Anti-leukemic effects of gallic acid on human leukemia K562 cells: Downregulation of COX-2, inhibition of BCR/ABL kinase and NF-κB inactivation. *Toxicology in Vitro*. 2012;**26(3)**:396–405. https://doi.org/10.1016/j.tiv.2011.12.018

13. Hwang EY, Huh J-W, Choi M-M, Choi SY, Hong H-N, Cho S-W. Inhibitory effects of gallic acid and quercetin on UDP-glucose dehydrogenase activity. *FEBS Letters*. 2008;**582(27)**:3793–3797. https://doi.org/10.1016/j.febslet.2008.10.010

14. Hseu Y-C, Chen S-C, Lin W-H, Hung D-Z, Lin M-K, Kuo Y-H, et al. Toona sinensis (leaf extracts) inhibit vascular endothelial growth factor (VEGF)-induced angiogenesis in vascular endothelial cells. *Journal of Ethnopharmacology*. 2011;**134(1)**:111–121. https://doi.org/10.1016/j.jep.2010.11.05

15. Ho H-H, Chang C-S, Ho W-C, Liao S-Y, Lin W-L, Wang C-J. Gallic acid inhibits gastric cancer cells metastasis and invasive growth via increased expression of RhoB, downregulation of AKT/small GTPase signals and inhibition of NF-κB activity. *Toxicology and Applied Pharmacology*. 2013;**266(1)**:76–85. https://doi.org/10.1016/j.taap.2012.10.019

16. You BR, Park WH. Gallic acid-induced lung cancer cell death is related to glutathione depletion as well as reactive oxygen species increase. *Toxicology in Vitro*. 2010;**24(5)**:1356–1362. https://doi.org/10.1016/j.tiv.2010.04.009

17. Lu Y, Jiang F, Jiang H, Wu K, Zheng X, Cai Y, et al. Gallic acid suppresses cell viability, proliferation, invasion and angiogenesis in human glioma cells. *European Journal of Pharmacology*. 2010;**641(2)**:102–107. https://ncbi.nlm.nih.gov/pmc/articles/PMC3003697/

18. Loreto C, Psaila A, Musumeci G, Castorina S, Leonardi R. Apoptosis activation in human carious dentin. An immunohistochemical study. *European Journal of Histochemistry: EJH*. 2015;**59(3)**. https://doi.org/10.4081/ejh.2015.2513

19. Tabas I, Ron D. Integrating the mechanisms of apoptosis induced by endoplasmic reticulum stress. *Nature Cell Biology*. 2011;**13(3)**:184–190. https://doi.org/10.1038/ncb0311-184

20. Obexer P, Geiger K, Ambros P, Meister B, Ausserlechner M. FKHRL1-mediated expression of Noxa and Bim induces apoptosis via the mitochondria in neuroblastoma cells. *Cell Death & Differentiation*. 2007;**14(3)**:534–547. https://doi.org/10.1038/sj.cdd.4402017

21. Benhusein GM, Mutch E, Aburawi S, Williams FM. Genotoxic effect induced by hydrogen peroxide in human hepatoma cells using comet assay. *Libyan Journal of Medicine*. 2010;**5(1)**. https://doi.org/10.3402/ljm.v5i0.4637

22. McKelvey-Martin VJ, Ho ET, McKeown SR, Johnston SR, McCarthy PJ, Rajab NF, et al. Emerging applications of the single cell gel electrophoresis (Comet) assay. I. Management of invasive transitional cell human bladder carcinoma. II. Fluorescent in situ hybridization Comets for the identification of damaged and repaired DNA sequences in individual cells. *Mutagenesis*. 1998;**13(1)**:1–8. https://doi.org/10.1093/mutage/13.1.1

23. Project E, Nachliel E, Gutman M. Force field-dependant structural divergence revealed during long time simulations of Calbindin d9k. *Journal of Computational Chemistry*. 2010;**31(9)**:1864–1872. https://doi.org/10.1002/jcc.21473

24. van der Spoel D, Berendsen HJ. Molecular dynamics simulations of Leu-enkephalin in water and DMSO. *Biophysical Journal*. 1997;**72(5)**:2032. https://doi.org/10.1016/s0006-3495(97)78847-7

25. JEYAM M, Grr K, Poornima V, Sharanya M. Molecular understanding and insilico validation of traditional medicines for Parkinson's disease. Asian *Journal of Pharmaceutical and Clinical Research*. 2012;**5(4)**:125–128. https://ajpcr.com/Vol3Issue4/104.pdf

26. Eskandari E, Heidarian E, Amini SA, Saffari-Chaleshtori J. Evaluating the effects of ellagic acid on pSTAT3, pAKT, and pERK1/2 signaling pathways in prostate cancer PC3 cells. 2016; **12(4)**:1266–1271. https://doi.org/10.4103/0973-1482.165873

27. Elmore S. Apoptosis: a review of programmed cell death. *Toxicologic Pathology*. 2007;**35(4)**:495–516. https://doi.org/10.1080/01926230701320337

28. Yeh R-D, Chen J-C, Lai T-Y, Yang J-S, Yu C-S, Chiang J-H, et al. Gallic acid induces G0/G1 phase arrest and apoptosis in human leukemia HL-60 cells through inhibiting cyclin D and E, and activating mitochondria-dependent pathway. *Anticancer Research*. 2011;**31(9)**:2821–2832. https://ncbi.nlm.nih.gov/pubmed/21868525

29. Ghasemi-Dehkordi P, Allahbakhshian-Farsani M, Abdian N, Mirzaeian A, Saffari-Chaleshtori J, Heybati F, et al. Comparison between the cultures of human induced pluripotent stem cells (hiPSCs) on feeder-and serum-free system (Matrigel matrix), MEF and HDF feeder cell lines. *Journal of Cell Communication and Signaling*. 2015;**9(3)**:233–246. https://doi.org/10.1007/s12079-015-0289-3

30. Allahbakhshian-Farsani M, Abdian N, Ghasemi-Dehkordi P, Sadeghiani M, Saffari-Chaleshtori J, Hashemzadeh-Chaleshtori M, et al. Cytogentic analysis of human dermal fibroblasts (HDFs) in early and late passages using both karyotyping and comet assay techniques. *Cytotechnology*. 2014;**66(5)**:815–822. https://doi.org/10.1007/s10616-013-9630-y

31. Olive PL, Banáth JP, Durand RE. Heterogeneity in radiation-induced DNA damage and repair in tumor and normal cells measured using the comet assay. *Radiation Research*. 1990;**122(1)**:86–94. https://doi.org/10.2307/3577587

32. Hanahan D, Weinberg RA. Hallmarks of cancer: the next generation. *Cell*. 2011;**144(5)**:646–674. https://doi.org/10.1016/j.cell.2011.02.013

33. Laubenbacher R, Hower V, Jarrah A, Torti SV, Shulaev V, Mendes P, et al. A systems biology view of cancer. *Biochimica et Biophysica Acta (BBA)-Reviews on Cancer*. 2009;**1796(2)**:129–139. https://doi.org/10.1016/j.bbcan.2009.06.001

34. Llambi F, Green DR. Apoptosis and oncogenesis: give and take in the BCL-2 family. *Current Opinion in Genetics & Development*. 2011;**21(1)**:12–20. https://doi.org/10.1016/j.gde.2010.12.001

35. Engel T, Henshall DC. Apoptosis, Bcl-2 family proteins and caspases: the ABCs of seizure-damage and epileptogenesis. *Int J Physiol Pathophysiol Pharmacol*. 2009;**1(2)**:97–115. https://ncbi.nlm.nih.gov/pubmed/21383882

36. Shamas-Din A, Brahmbhatt H, Leber B, Andrews DW. BH3-only proteins: orchestrators of apoptosis. *Biochimica et Biophysica Acta (BBA)-Molecular Cell Research*. 2011;**1813(4)**:508–520. https://doi.org/10.1016/j.bbamcr.2010.11.024

37. Wen X, Lin ZQ, Liu B, Wei YQ. Caspase-mediated programmed cell death pathways as potential therapeutic targets in cancer. *Cell Proliferation*. 2012;**45(3)**:217–224. https://doi.org/10.1111/j.1365-2184.2012.00814.x

38. Sambantham S, Radha M, Paramasivam A, Anandan B, Malathi R, Chandra SR, et al. Molecular mechanism underlying hesperetin-induced apoptosis by in silico analysis and in prostate cancer PC-3 cells. *Asian Pac J Cancer Prev*. 2013;**14(7)**:4347–4352. https://doi.org/10.7314/apjcp.2013.14.7.4347

39. Chaleshtori JS, Soreshjani EH, Reisi F, Tabatabaiefar MA, Asadi-Samani M, Zamanian N, et al. Damage intensity of carvacrol on prostate cancer cells and its effects on molecular dynamic simulation of apoptotic factors. *Int J Pharmtech Res*. 2016;**9(6)**:261–273. http://sphinxsai.com/2016/ph_vol9_no6/abstracts/A(261-273)V9N6PT.pdf

40. Saffari-Chaleshtori J, Heidari-Soreshjani E, Asadi-Samani M. Computational study of quercetin effect on pre-apoptotic factors of Bad, Bak and Bim. *Journal of HerbMed Pharmacology*. 2016;**5(2)**:61–66. http://herbmedpharmacol.com/Abstract/JHP_20160324163221